



HAL
open science

The heavy atom substitution and semi-experimental equilibrium structures of 2-ethylfuran obtained by microwave spectroscopy

Ha Vinh Lam Nguyen

► **To cite this version:**

Ha Vinh Lam Nguyen. The heavy atom substitution and semi-experimental equilibrium structures of 2-ethylfuran obtained by microwave spectroscopy. *Journal of Molecular Structure*, 2020, 1208, pp.127909. 10.1016/j.molstruc.2020.127909. hal-03181947

HAL Id: hal-03181947

<https://hal.u-pec.fr/hal-03181947>

Submitted on 26 Mar 2021

HAL is a multi-disciplinary open access archive for the deposit and dissemination of scientific research documents, whether they are published or not. The documents may come from teaching and research institutions in France or abroad, or from public or private research centers.

L'archive ouverte pluridisciplinaire **HAL**, est destinée au dépôt et à la diffusion de documents scientifiques de niveau recherche, publiés ou non, émanant des établissements d'enseignement et de recherche français ou étrangers, des laboratoires publics ou privés.

The heavy atom substitution and semi-experimental equilibrium structures of 2-ethylfuran obtained by microwave spectroscopy

Ha Vinh Lam Nguyen*

Laboratoire Interuniversitaire des Systèmes Atmosphériques (LISA), CNRS UMR 7583, Université Paris-Est Créteil, Université de Paris, Institut Pierre Simon Laplace, 61 avenue du Général de Gaulle, 94010 Créteil, France.

Email: lam.nguyen@lisa.u-pec.fr

* For Jon and our memories.

Abstract

The substitution r_s and semi-experimental equilibrium r_e^{SE} structures of the two conformers of 2-ethylfuran were obtained using a combination of microwave spectroscopy and quantum chemistry. The microwave spectrum was recorded using a molecular jet Fourier-transform spectrometer operating in the frequency range of 2.0 GHz to 26.5 GHz. The spectra of all ^{13}C and ^{18}O isotopologues of both conformers could be measured in their natural abundances and the experimental gas-phase heavy atom structures were determined. All spectra were fitted using a semi-rigid rotor model including centrifugal distortion correction. The molecular geometries were compared with those of related molecules within the frame of the current literature. This work indicated that in some cases, the time required for recording survey scans of a Fourier-transform resonator setup can be reduced significantly with supports from adequate quantum chemical methods and spectral analysis skill.

Keywords: rotational spectroscopy, microwave structure, structure determination, conformational analysis

1. Introduction

The title compound, 2-ethylfuran (2EF), with the structure given in Figure 1, belongs to the class of heteroaromatic organic compounds. It is a derivative of furan used in fragrances for rum and cocoa notes [1]. 2EF is also a natural component of various plant species and numerous cooked foods and drinks, e.g. beef, chicken, pork liver, rice, soybean, oats, tea, and coffee [1]. With its ethereal taste and its sweet and burnt odor which strongly reminds one of coffee, chocolate, and rum, 2EF is widely used as a flavoring ingredient, such as in bakery at 40 ppm, desserts at 20 ppm, soft drinks at 12 ppm, and alcoholic beverage at 3 ppm [2].

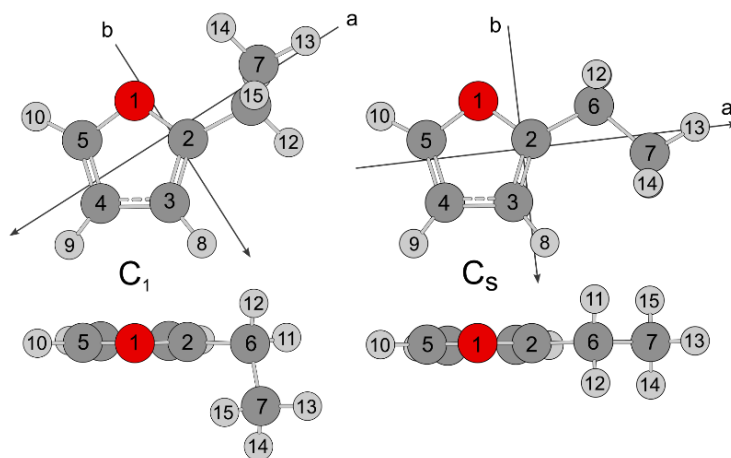


Figure 1. Molecular structures of the two conformers (C_1 and C_s) of 2EF obtained from calculations at the MP2/6-31G(d,p) level of theory in their principal axis of inertia.

2EF fits well in a series of flavor molecules containing a five-membered ring whose gas-phase structures have been previously studied by the author and co-workers. They are for example 2-methyltetrahydrothiophene (natural flavor in Petite Arvine wine and Chinese brandy) [3], 5-methyl furfural (flavoring agent with almond odor) [4], 2-acetyl-5-methylfuran (natural flavor in Chinese liquors, smoked salmon, and roasted coffee beans) [5], 2-methylpyrrole (fried chicken) [6], and most recently coffee furanone (coffee aroma, natural flavor in tomatoes and pork) [7]. However, the flavor or scent of 2EF is not the only reason for the author to study this particular molecule. Conformational analysis has always been the subject of interest for the microwave spectroscopic community. There are also a considerable number of molecules containing five-membered aromatic heterocycles which have been investigated by this technique, such as furans [8-10], thiophenes [11-13], thiazoles [14-16], isothiazoles [17,18], oxazoles [19-21], isoxazoles [22,23], oxadiazole [17,24-26], pyrroles [6,27,28], and imidazoles [17,29,30]. 2EF conjoins the

conformational landscape arising from the orientation of the ethyl group with a relatively rigid furan ring.

It is known that if an ethyl group is attached to a frame with C_s symmetry, it prefers two orientations: One with the ethyl C-C bond also lying on the plane of the frame (the in-plane or C_s conformer) and one with the methyl group of the ethyl moiety tilted out of that plane (the out-of-plane, *gauche*, or C_1 conformer) [31-35]. In a study on ethyl valerate, Mouhib et al. pointed out that the values of the rotational constants of the C_1 conformer calculated at the MP2/6-31G(d,p) level of theory were closest to the experimentally deduced values [36]. Further studies on some anisole derivatives also suggested this level for predicting rotational constants in molecules containing an aromatic ring [37,38]. Other works on aromatic five-membered rings with C_s symmetry, on the other hand, have shown that the combination of the MP2 method with the 6-311++G(d,p) basis set yielded rotational constants which were in good agreement with the experimental values [4,5,9,12]. This level has also given reliable results for many other classes of compounds [39-42], and thus has become one of the level most frequently used by the author. Based on the results of previous works, it was almost obvious to guess that 2EF would possess two conformers, one with all co-planar heavy atoms and one with C_1 symmetry where the methyl group tilts out of the furan plane. The author was interested in testing and validating this assumption. The experimentally determined structures will be compared with those of other furan derivatives.

The rapid development and increasing population of molecular jet chirped pulse Fourier transformed microwave (FTMW) spectrometers since it was first introduced a decade ago [43] have indicated a drawback of the classical resonator FTMW setup, which is the higher amount of time required for recording broadband scans. But how much is the time needed for the survey spectrum of 2EF? The present work will show that the time requirement for survey spectra of a classical resonator spectrometer can be reduced in some cases if adequate quantum chemical methods and spectral analysis technique are applied to support the measurements.

2. Quantum chemical calculations

Due to the rigidity of the furan frame in 2EF, the rotation of the ethyl group is the only degree of freedom to generate different minima on the potential energy surface. Figure 2 illustrates the potential energy curves obtained by rotating this group in steps of 10° by varying the dihedral angle $\varphi = \angle(O1,C2,C6,C7)$ while all other geometry parameters were allowed to relax during

optimizations (for atom numbering, see Figure 1). Calculations were carried out at the MP2/6-311++G(d,p) and MP2/6-31G(d,p) levels of theory using the *Gaussian 16* program package [44]. The calculated energies were parameterized using a Fourier expansion with the coefficients given in Table S-1 of the supplementary material. Both potential energy curves show three energy minima, which correspond to a conformer with all heavy atom located on a molecular plane at $\varphi = 180^\circ$ (henceforward called the C_s conformer) and a conformer with the methyl group tilted out of the furan plane by about 60° (called the C_1 conformer) and its mirror image at $\varphi \approx 300^\circ$. The two structures at $\varphi = 180^\circ$ and $\varphi \approx 300^\circ$ were re-optimized to allow full structural relaxation. The geometries from full optimizations at the MP2/6-31G(d,p) level of theory are depicted in Figure 1; the Cartesian coordinates of both conformers are available in Table S-2 of the supplementary material; the *ab initio* results are summarized in Table 1. The C_1 conformer is predicted as the global minimum structure. The relative energy differences between the two conformers calculated at the MP2/6-311++G(d,p) and the MP2/6-31G(d,p) levels including zero-point energy corrections are $1.74 \text{ kJ}\cdot\text{mol}^{-1}$ and $1.92 \text{ kJ}\cdot\text{mol}^{-1}$, respectively. While the values of the dipole moment components in *b*- and *c*-direction predicted at both levels agree well, there are significant differences in the value of the *a*-dipole moment component for both conformers. As will be shown in the experimental and the discussion sections, the 6-31G(d,p) basis set is not appropriate for the calculation of dipole moments.

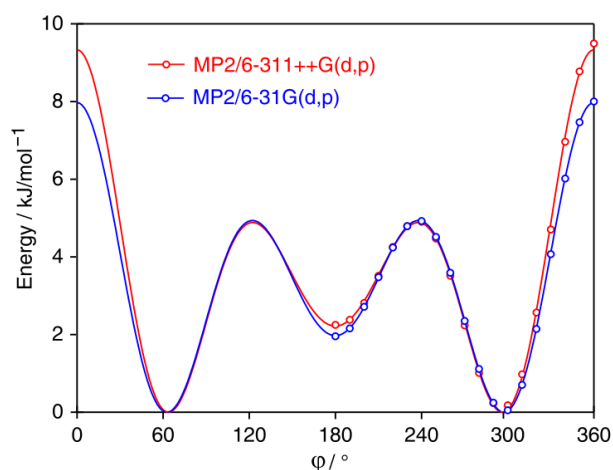


Figure 2. Potential energy curves of 2EF obtained by rotating the ethyl group. The dihedral angle $\varphi = \angle(\text{O1}, \text{C2}, \text{C6}, \text{C7})$ was varied in steps of 10° , and the geometries were optimized at the MP2/6-311++G(d,p) (red curve) and MP2/6-31G(d,p) (blue curve) levels of theory. Two stable conformers are found at 180° (C_s symmetry) and about $\pm 60^\circ$ (image and mirror image, C_1 symmetry).

Table 1. Equilibrium rotational constants A_e , B_e , C_e (in MHz), vibrational ground state rotational constants A_0 , B_0 , C_0 (in MHz) and centrifugal distortion constants (in kHz) in the symmetrically reduced Hamiltonian obtained from anharmonic frequency calculations, dipole moment components μ (in Debye), relative electronic energies ΔE (in $\text{kJ}\cdot\text{mol}^{-1}$) with respect to the lowest energy C_1 conformer, and relative electronic energies including the zero-point energy corrections ΔE_{ZPE} (in $\text{kJ}\cdot\text{mol}^{-1}$) calculated at the MP2/6-311++G(d,p) and MP2/6-31G(d,p) levels of theory.

	MP2/6-311++G(d,p)		MP2/6-31G(d,p)	
	C_1	C_s	C_1	C_s
A_e	6648.1	7064.4	6682.2	7084.7
B_e	1950.9	1937.1	1957.5	1939.3
C_e	1660.3	1549.6	1660.1	1551.6
A_0	6615.0	7011.0	6621.5	7032.7
B_0	1932.2	1917.5	1941.9	1920.5
C_0	1644.6	1537.1	1650.0	1539.0
D_J	0.33240	0.15058	0.31688	0.14506
D_{JK}	2.37323	-0.02336	2.34152	-0.02198
D_K	3.22064	1.77121	2.95765	1.77015
d_1	-0.02514	-0.03562	-0.02853	-0.03546
d_2	-0.00148	0.00106	-0.00415	-0.00127
μ_a	-0.20	0.55	-0.01	0.38
μ_b	0.67	0.62	0.65	0.64
μ_c	0.12	0.00	0.13	0.00
ΔE	0.0	2.14	0.0	1.93
ΔE_{ZPE}	0.0	1.74	0.0	1.92

3. Microwave spectroscopy

3.1. Measurements

2EF was purchased from TCI Europe, Zwijndrecht, Belgium. To record the microwave spectrum, a gas mixture of 1% 2EF in helium at a total pressure of 75-120 kPa was expanded through a pulsed nozzle into the cavity. Helium was chosen over argon or neon because of the warmer supersonic jet that enables the observation of high J transitions and consequently accurate centrifugal distortion constants. All spectra were recorded using a FTMW spectrometer operating in the frequency range from 2.0 to 26.5 GHz [45]. The broadband scans of the parent species consist of automatically taken overlapping spectra at a step width of 0.25 MHz with 30 co-added decays per

each spectrum. The instrumental accuracy for isolated lines recorded under high resolution is approximately 2 kHz [46].

3.2. Spectral assignments and fits

3.2.1. The C₁ conformer

For the spectral assignment, the author started with the C₁ conformer with the rotational constants $A = 6682$ MHz, $B = 1958$ MHz, and $C = 1660$ MHz obtained at the MP2/6-31G(d,p) level of theory. From the predicted dipole moment components given in Table 1, the spectrum of this conformer should be dominated by *b*-type transitions, accompanied by weaker *c*-type transitions, and *a*-type transitions were expected to be too weak for observation.

The author first looked for the *b*-type $3_{13} \leftarrow 2_{02}$ transition predicted at 14839.3 MHz with a survey spectrum of ± 30 MHz around the predicted frequency. The scan was stopped after an intense line was found at 14834.75 MHz, and the next transition $2_{12} \leftarrow 1_{01}$ of the same *R*-branch was searched. After the first scan had given the author confidence on the calculated rotational constants in use, the next scan was started at 11650 MHz, about 10 MHz earlier than the predicted frequency of 11661.2 MHz. After the line was found at 11662.75 MHz, the scan was stopped and the third scan to search for the $4_{14} \leftarrow 3_{03}$ transition predicted at 17890.2 MHz was started at 17880 MHz. This transition was found at 17883 MHz, allowing together with other two previously observed transitions a fit which had fixed all three rotational constants. The fourth transition $3_{22} \leftarrow 3_{13}$ was found straightforwardly at 15557 MHz with the prediction from the fitted rotational constants (the frequency predicted from *ab initio* was 15520.6 MHz) and further transitions were measured afterwards. The *b*-type transitions were the strongest, and as expected, the *c*-type ones were much weaker. Surprisingly, *a*-type transitions were almost as intense as the *b*-type ones.

Altogether, 35 *a*-type, 67 *b*-type, and 6 *c*-type lines with $J \leq 19$ and $K_a \leq 5$ were fitted using a program written by the author for Separately Fitting of Large Amplitude Motion Species (*SFLAMS*). For a semi-rigid rotor, as in the case of 2EF, the Hamiltonian only contains rotational and quartic centrifugal distortion terms using Watson's S reduction. The observed frequency list is given in Table S-3 in the supplementary material; the spectroscopic parameters are summarized in Table 2.

Table 2. Molecular parameters of the parent species, as well as the ^{13}C and ^{18}O isotopologues of the C_1 conformer of 2EF obtained from the *SFLAMS* fits. Atoms are numbered according to Figure 1.

Par. ^a	Unit	^{12}C	$^{13}\text{C}(2)$	$^{13}\text{C}(3)$	$^{13}\text{C}(4)$	$^{13}\text{C}(5)$	$^{13}\text{C}(6)$	$^{13}\text{C}(7)$	$^{18}\text{O}(1)$
A_0	MHz	6693.72695(15)	6682.26778(82)	6570.8614(16)	6671.19127(69)	6630.3850(13)	6657.6487(15)	6660.8953(11)	6523.10957(42)
B_0	MHz	1947.754374(30)	1947.22110(23)	1943.22833(35)	1918.06890(16)	1927.27946(27)	1925.86239(33)	1899.44059(28)	1945.18414(22)
C_0	MHz	1656.347742(31)	1655.80936(19)	1645.51033(30)	1634.19012(13)	1637.69490(23)	1640.96918(27)	1622.34763(23)	1645.14961(13)
D_J	kHz	0.31569(25)	0.3085(38)	0.3107(57)	0.3071(27)	0.3098(43)	0.3112(55)	0.3051(48)	0.0 ^b
D_{JK}	kHz	2.1943(11)	2.150(13)	2.258(22)	2.123(11)	2.127(15)	2.084(21)	2.134(18)	0.0 ^b
D_K	kHz	2.789(15)	2.99(18)	2.42(35)	2.52(15)	2.33(26)	2.53(31)	3.11(24)	0.0 ^b
d_I	kHz	-0.028635(50)	-0.0271(11)	-0.0322(19)	-0.02314(80)	-0.0293(15)	-0.0271(17)	-0.0284(14)	0.0 ^b
d_2	kHz	0.000863(22)	0.000863 ^c	0.000863 ^c	0.00226(41)	0.000863 ^c	0.00146(81)	-0.00140(71)	0.0 ^b
rms^d	kHz	1.3	1.9	2.8	1.2	2.1	2.5	2.2	1.4
N^e		108	26	21	22	23	23	25	6

^a All parameters refer to the principal axis system. Watson's S reduction and I' representation were used.

^b Not possible to be fitted or to be fixed to the value of the parent species due to the small number of lines. Fixed to zero.

^c Fixed to the value of the parent species.

^d Root-mean-square deviation of the fit.

^e Number of lines.

Table 3. Molecular parameters of the parent species, as well as the ^{13}C and ^{18}O isotopologues of the C_s conformer of 2EF obtained from the *SFLAMS* fits. Atoms are numbered according to Figure 1.

Par. ^a	Unit	^{12}C	$^{13}\text{C}(2)$	$^{13}\text{C}(3)$	$^{13}\text{C}(4)$	$^{13}\text{C}(5)$	$^{13}\text{C}(6)$	$^{13}\text{C}(7)$	$^{18}\text{O}(1)$
A_0	MHz	7104.81359(20)	7102.97341(91)	6985.97511(84)	7020.94141(71)	7089.0064(18)	7061.08572(94)	7086.16188(81)	6.8831842(20)
B_0	MHz	1933.284765(51)	1933.06076(28)	1932.57454(25)	1910.95621(21)	1905.23416(42)	1914.44973(28)	1882.84724(24)	1.92447193(53)
C_0	MHz	1549.965675(48)	1549.73989(19)	1.54377919(17)	1531.62128(15)	1531.15234(35)	1535.78830(20)	1516.53197(18)	1.53354897(49)
D_J	kHz	0.14347(59)	0.1419(27)	0.1434(25)	0.1432(21)	0.1389(34)	0.1351(28)	0.1409(24)	0.1321(52)
D_{JK}	kHz	0.0040(14)	0.004046 ^b						
D_K	kHz	1.906(27)	2.20(23)	1.39(21)	1.61(18)	1.37(43)	2.38(24)	2.30(21)	1.906 ^b
d_1	kHz	-0.035310(64)	-0.0337(32)	-0.0346(30)	-0.0367(26)	-0.0348(47)	-0.0331(35)	-0.0357(30)	-0.0274(59)
d_2	kHz	-0.002519(27)	-0.002519 ^b						
rms^c	kHz	1.3	1.3	1.2	1.1	1.7	1.4	1.2	1.6
N^d		96	24	25	25	24	26	25	13

^a All parameters refer to the principal axis system. Watson's S reduction and I' representation were used.

^b Fixed to the value of the parent species.

^c Root-mean-square deviation of the fit.

^d Number of lines.

3.2.2. The C_s conformer

For conformers with all heavy atoms located on a symmetry plane, the MP2/6-311G++(d,p) level of theory has proven its reliability in calculating rotational constants of aromatic five-membered rings for assignment purposes [4,5,9,12]. Therefore, the rotational constants calculated at this level were used to predict the microwave spectrum of the C_s conformer of 2EF. Due to symmetry, no *c*-type transitions were expected. From the calculated dipole moment components, *a*- and *b*-type transitions should be similarly intense. Therefore, the author searched for the $3_{13} \leftarrow 2_{12}$, $3_{12} \leftarrow 2_{11}$, and $4_{14} \leftarrow 3_{13}$ *a*-type transitions. The assignment process was similar to that of the C₁ conformer, and the lines predicted at 9866 MHz, 11028 MHz, and 13131 MHz, respectively, were found at 9862 MHz, 11012 MHz, and 13127 MHz. Fitting these three lines had fixed all rotational constants, and helped to predict and measure 46 further *a*-type and 50 *b*-type lines with $J \leq 18$ and $K_a \leq 6$ directly in the high resolution mode of the spectrometer. The observed frequency list is given in Table S-4 of the supplementary material; the spectroscopic parameters are summarized in Table 3.

3.2.3. The ¹³C isotopologues

In previous studies on three molecules related to 2EF, coffee furanone [7], 2-methyltetrahydrofuran [47], and 2-thiophenecarboxaldehyde [48], the spectra of ¹³C isotopologues in natural abundances of about 1% could be observed using the same instrumental setup. The author thus assumed that it was also the case for 2EF and had calculated the isotopic shifts of all ¹³C isotopologues of the C₁ and C_s conformers. The assignments of ¹³C isotopologue spectra of the C_s conformer were straightforward by searching for the same three *a*-type transitions mentioned in section 3.2.2. Small scans of ± 2 MHz around the isotopic shift corrected frequencies (given in Table S-5 in the supplementary material) were performed with step widths of 0.25 MHz and 100 co-added decays per each measurement. After fitting these three transitions, the fourth transition $3_{03} \leftarrow 2_{02}$ and then further transitions with $J \leq 6$ and $K_a \leq 3$ could be found directly in the high resolution mode. The rotational constants were deduced, and three quartic centrifugal distortion constants could also be determined. The spectroscopic parameters are given in Table 3; the frequency lists are available in Table S-3 of the supplementary material.

For the C₁ conformer, the assignments of the ¹³C isotopologues followed the same manner as for the C_s conformer, but required trial and error in some cases. Transitions with $J \leq 7$ and $K_a \leq 2$ could be measured and fitted to determine accurately the rotational constants and at least four

quartic centrifugal distortion constants. The results of the fits are summarized in Table 2, and the frequency lists are given in Table S-2 of the supplementary material.

3.2.4. The ^{18}O isotopologue

To complete the heavy atom structure, the author searched for the ^{18}O -isotopologue of both conformers. Because of its low natural abundance of 0.2 %, scans of ± 2 MHz around the predicted frequencies of the same transitions as those used to assign the spectra of the ^{13}C isotopologues were performed by steps of 0.2 MHz with 500 co-added decays at each step. In total, only 6 lines could be measured for the C_1 conformer, and none of the quartic centrifugal distortion constants could be fitted. Fixing them to the values of the parent species, as having been done for other isotopologues, led to an rms deviation of 21.3 kHz. Therefore, they had to be fixed to zero. For the C_s conformer, two centrifugal distortion constants were determined, and the others three were fixed to the values of the parent species.

3.3. Microwave structure determinations

3.3.1. The substitution r_s structures

Using the experimental rotational constants of the parent species and the ^{13}C and ^{18}O -isotopologues, the heavy atom microwave structures of both conformers, C_s and C_1 , of 2EF were determined with Kraitchman's equations [49] using the programs KRA and EVAL available at the PROSPE website [50]. Costain's rule was used to calculate the uncertainties [51]. The signs of the atom coordinates were taken from the geometries calculated by *ab initio*. The atom coordinates given by the program KRA, the bond lengths, bond angles, and dihedral angles given by the program EVAL are presented in Tables 4 and 5. For the C_s conformer, the values of the c -coordinates were smaller than the errors of the calculations, indicating that they could not be determined, and therefore were fixed to zero.

Table 4. Experimental atom positions (substitution r_s and semi-experimental equilibrium r_e^{SE} geometries) of the two conformers of 2EF obtained by isotopic substitutions with Kraitchman’s equations [49] as implemented in the program KRA [50]. For the C_s conformer, all c -coordinates were set to zero due to planarity. For comparison, the equilibrium atom positions (r_e geometry) obtained from optimizations at the MP2/6-31G(d,p) level of theory are presented.

	C₁ conformer						C_s conformer					
	$r_{0 \rightarrow e}^{SE}$			r_e			$r_{0 \rightarrow e}^{SE}$			r_e		
	$a/\text{Å}$	$b/\text{Å}$	$c/\text{Å}$	$a/\text{Å}$	$b/\text{Å}$	$c/\text{Å}$	$a/\text{Å}$	$b/\text{Å}$	$c/\text{Å}$	$a/\text{Å}$	$b/\text{Å}$	$c/\text{Å}$
O(1)	0.3351(72)	-0.9673(25)	-0.2452(31)	0.32097	-0.97123	-0.24871	-0.7825(16)	-1.0820(11)	-0.00015	-0.78108	-1.08712	-0.00015
C(2)	-0.184(12)	0.284(39)	-0.2199(39)	-0.19638	0.30100	-0.22152	0.2172(80)	-0.1548(82)	0.00001	0.22060	-0.14881	0.00001
C(3)	0.7754(53)	1.1912(39)	0.0871(41)	0.79637	1.19157	0.09027	-0.3200(67)	1.0994(20)	-0.00011	-0.32760	1.10672	-0.00011
C(4)	1.9913(24)	0.4392(65)	0.2615(22)	1.99411	0.43420	0.26086	-1.7401(13)	0.9380(22)	-0.00001	-1.74566	0.93755	-0.00001
C(5)	1.6511(25)	-0.8588(56)	0.0472(29)	1.65208	-0.87013	0.04623	-1.9653(12)	-0.4023(42)	0.00020	-1.96827	-0.40903	0.00020
C(6)	-2.5110(17)	-0.2973(82)	0.5454(58)	-1.65379	0.42289	-0.49336	1.6112(14)	-0.6763(27)	-0.00001	1.61461	-0.67417	-0.00001
C(7)	-1.875(14)	0.0283(91)	-1.476(34)	-2.50951	-0.29756	0.54964	2.64138(76)	0.4479(41)	0.00009	2.64991	0.44530	0.00009
H(8) ^a	0.630(18)	2.250(54)	0.1725(71)	0.67766	2.25827	0.18145	0.214(26)	1.998(17)	-0.00020	0.21615	2.03587	-0.00020
H(9) ^a	2.965(49)	0.815(24)	0.509(14)	2.97514	0.80194	0.50885	-2.467(16)	1.690(17)	-0.00001	-2.49824	1.70745	-0.00001
H(10) ^a	2.197(28)	-1.782(46)	0.0601(64)	2.19977	-1.79558	0.05973	-2.829(19)	-0.992(13)	0.00037	-2.85484	-1.01782	0.00037
H(11) ^b	-1.875(14)	0.0283(91)	-1.476(35)	-1.87348	0.02654	-1.48768	1.7536(47)	-1.3080(34)	-0.86365(23)	1.75721	-1.31411	-0.87439
H(12) ^b	-1.8878(80)	1.472(52)	-0.5133(79)	-1.89787	1.48607	-0.51541	1.7536(47)	-1.3082(34)	0.86353(23)	1.75719	-1.31425	0.87427
H(13) ^b	-3.562(43)	-0.183(15)	0.323(12)	-3.57005	-0.19042	0.32458	3.6428(14)	0.0449(64)	0.00008	3.65779	0.03430	0.00008
H(14) ^b	-2.2781(80)	-1.352(48)	0.563(22)	-2.26749	-1.35829	0.57029	2.5293(19)	1.0709(38)	-0.87430(23)	2.53969	1.07430	-0.88202
H(15) ^b	-2.324(11)	0.105(13)	1.531(40)	-2.32457	0.11201	1.54161	2.5292(19)	1.0708(38)	0.87457(23)	2.53966	1.07417	0.88228
	r_s			$r_{s \rightarrow e}^{SE}$			r_s			$r_{s \rightarrow e}^{SE}$		
O(1)	0.3348(45)	-0.9712(16)	-0.2527(60)	0.3342(45)	-0.9622(16)	-0.2684(56)	-0.7766(19)	-1.0839(14)	0.0	-0.7831(20)	-1.0809(14)	0.0
C(2)	-0.143(11)	0.2816(54)	-0.2261(67)	-0.124(13)	0.2622(58)	-0.2712(56)	0.1729(89)	-0.134(12)	0.0	0.2129(71)	-0.150(10)	0.0
C(3)	0.7750(20)	1.1929(13)	0.059(26)	0.7764(20)	1.1845(13)	0.1418(11)	-0.3105(49)	1.1043(14)	0.0	-0.3081(49)	1.0988(14)	0.0
C(4)	1.99287(75)	0.4396(35)	0.2623(58)	1.99141(75)	0.4209(36)	0.2813(54)	-1.75009(86)	0.9328(17)	0.0	-1.74164(86)	0.9339(17)	0.0
C(5)	1.66247(90)	-0.8579(18)	0.037(41)	1.64882(91)	-0.8474(18)	0.1811(83)	-1.96778(76)	-0.4030(38)	0.0	-1.96560(76)	-0.3989(38)	0.0
C(6)	-1.64732(91)	0.4027(38)	-0.5052(30)	-1.65195(91)	0.3900(39)	-0.5173(29)	1.60712(93)	-0.6696(23)	0.0	1.61203(93)	-0.6731(23)	0.0
C(7)	-2.51888(60)	-0.2938(52)	0.5471(28)	-2.51014(60)	-0.2782(54)	0.5562(27)	2.65413(57)	0.4413(34)	0.0	2.64213(57)	0.4416(34)	0.0

^a The atom locations were varied in the fitting to obtain the $r_{0 \rightarrow e}^{SE}$ coordinates. The bond lengths to the carbon atom of the ring were constrained to be the same.

^b The atom locations were varied in the fitting to obtain the $r_{0 \rightarrow e}^{SE}$ coordinates. The bond lengths to the carbon atom of the CH_2CH_3 moiety were constrained to be the same.

Table 5. Experimental structure parameters (bond lengths, bond angles, and dihedral angles) deduced from the substitution r_s and semi-experimental equilibrium $r_{s \rightarrow e}^{SE}$ geometries of the two conformers of 2EF using the program EVAL [50].

	C₁		C_s	
	r_s	$r_{s \rightarrow e}^{SE}$	r_s	$r_{s \rightarrow e}^{SE}$
Bond lengths / Å				
O1–C2	1.3412(66)	1.3072(72)	1.343(11)	1.3631(88)
C2–C3	1.323(10)	1.3535(98)	1.329(12)	1.3534(99)
C3–C4	1.4464(45)	1.4418(29)	1.4498(49)	1.4430(50)
C4–C5	1.3578(78)	1.3175(40)	1.3534(40)	1.3515(41)
O1–C5	1.3636(99)	1.3941(54)	1.3720(27)	1.3651(27)
C2–C6	1.535(11)	1.553(12)	1.5310(91)	1.4936(76)
C6–C7	1.5336(41)	1.5282(41)	1.5265(31)	1.5178(31)
Bond angles / °				
O1–C2–C3	113.56(77)	113.86(86)	113.69(67)	110.42(54)
C2–C3–C4	104.82(40)	103.25(45)	104.53(44)	106.08(38)
C3–C4–C5	105.63(43)	106.46(15)	106.05(11)	106.10(11)
C4–C5–O1	110.59(19)	110.43(20)	110.50(14)	110.44(15)
O1–C2–C6	114.80(57)	114.98(65)	114.51(76)	116.46(69)
C3–C2–C6	131.63(50)	130.30(54)	131.80(77)	133.12(68)
C2–C6–C7	113.35(32)	113.91(30)	112.83(44)	112.26(41)
Dihedral angles / °				
O1–C2–C6–C7	63.31(64)	62.30(59)	180 ^a	180 ^a
C3–C2–C6–C7	–115.5(16)	–106.25(81)	0 ^a	0 ^a

^a Derived from setting all experimental c -coordinates to zero.

3.3.2. The semi-experimental equilibrium r_e^{SE} structures

The r_s structure determination given in Section 3.3.1. is one of the most frequently applied method to determine experimental gas phase structures, especially in earlier studies when calculation capacity was still limited or if only a small number of isotopic species is available. The rotational constants of the vibrational ground state derived from the microwave spectra are used directly without any correction. Therefore, the r_s structure cannot be compared with the equilibrium r_e structure. The influence of vibrations also decreases the accuracy while comparing geometry parameters between different molecules. With the rapid development of computational capacity

and increasing precision of computational methods over the last decades, several alternatives have been proposed to overcome the problems of the r_s structure, one of them is the semi-experimental equilibrium r_e^{SE} structure. Several studies in the literature have indicated the general acceptance of the r_e^{SE} structure as a reasonable choice for structure determination [26,52-54].

The r_e^{SE} structure can be determined with two methods. The first method employs a “corrected r_s structure” where the experimental rotational constants $A_{0,exp.}$, $B_{0,exp.}$, and $C_{0,exp.}$ of the parent species and all isotopologues input in the program KRA [50] are corrected using the rovibrational corrections calculated from the *ab initio* cubic force field, resulting in the so-called $r_{s \rightarrow e}^{SE}$ structure (see Table S-6 in the supplementary material). However, in the case of 2EF where only information obtained from the spectra of heavy atoms is available, a complete structure determination is not possible because no statements can be made about the hydrogen atom locations. Nevertheless, hydrogen coordinates from *ab initio* calculations can be taken together with the vibrationally corrected experimental constants of all observed isotopologues to generate a least-squares fit structure using the program STRFIT [55], resulting in the so-called $r_{0 \rightarrow e}^{SE}$ structure. With this second method, the internal coordinates are varied until the sum of the squared deviations from the moments of inertia of all experimentally observed isotopologues is minimum. All hydrogen atom locations were allowed to vary in the fitting, but the C–H bond lengths of three hydrogen atoms attached to the furan ring, as well as those of the five hydrogen atoms in the CH₂CH₃ moiety are constrained to be the same. The r^{SE} structures of both, the C₁ and the C_s conformer of 2EF, are also given in Tables 4 and 5. The final results of STRFIT are available in Table S-7 of the supplementary material. All anharmonic frequency calculations were performed at the more cost-efficient MP2/6-31G(d,p) level of theory.

4. Discussion

The microwave spectra of two conformers of 2EF were assigned together with those of all ¹³C and ¹⁸O-isotopologues and fitted to root-mean-square deviations close to the experimental accuracy of 2 kHz. The rotational constants and quartic centrifugal distortion constants are well-determined for the parent species. Values of the experimental rotation constants of both conformers are in good agreement with those of the equilibrium constants predicted at the MP2/6-31G(d,p) level presented in Table 1. Though this agreement is most likely due to error compensations, because the MP2/6-31G(d,p) level of theory is less accurate than the higher level MP2/6-311++G(d,p), it provides a

reasonable compromise between calculation time and accuracy for spectral assignment purposes, and is therefore recommended for molecules with an ethyl group attached to a planar group/aromatic ring like 2EF.

Only a very limited number of investigations on the structure determination of furan derivatives has been reported in the literature, probably because of the low natural abundance of the ^{18}O isotopologue (0.2%) which often inhibits a complete heavy atom structure determination. Except for furan (**1**) [8,52], whose complete structure was determined prior to 2EF (**2**), there is only one structure determination study on a furan derivative, furfural (**3**), which exists as an *anti* and a *syn* conformer [56] (for molecule numbering, see Figure 3). Comparison of bond lengths and bond angles of the C_1 and C_s conformers of 2EF (**2**) as well as of the *anti* and *syn* conformers of furfural (**3**) shown in Figure 3 indicates that the ring structure is essentially unchanged upon conformation. Comparing the structural parameters of 2EF (**2**) with those of furfural (**3**) confirms that the ring structure also remains very similar in both molecules, though in 2EF (**2**) a substitution with +I effect (the ethyl group) is attached at the C(2) atom, while in furfural (**3**), the formyl group features –I effect. This indicates that electronic effect is of minor importance for the molecular structure of the furan ring. On the other hand, substitution alters the geometry parameters at the substituted position. Comparison of the O1–C2 and C2–C3 bond lengths as well as the O1–C2–C3 bond angle of 2EF (**2**) and furfural (**3**) with those of furan (**1**) shows that the O1–C2–C3 angle becomes about 3° larger with the presence of a substitution at the C(2) atom. Consequently, the O1–C2 and C2–C3 bond lengths are shorter in 2EF (**2**) and furfural (**3**) than they are in furan (**1**). There are further investigations on furan derivatives, such as those on fural-3-carboxaldehyde [57], 2-furancarbonitrile [58], furfuryl alcohol [59], furfuryl mercaptan [60], and 2-vinyl furan [61], but no structure determination has been reported and only geometry parameters calculated by quantum chemistry are presented.

An investigation on furfurylamine with a partial r_s structure is available, where Hedgecock et al. reported a dihedral angle $\angle(\text{O1},\text{C2},\text{C6},\text{N7})$ of $65.37(23)^\circ$, but the structure of the furan ring had been taken from a previous work [62]. This value is very similar to the value of $63.3(7)^\circ$ found for the dihedral angle $\angle(\text{O1},\text{C2},\text{C6},\text{C7})$ of the C_1 conformer of 2EF. The angles of 62.5° and 64.3° calculated at the MP2/6-31G(d,p) and the MP2/6-311++G(d,p) level of theory, respectively, are both very close to the experimental value. In a microwave study on ethylbenzene, only one conformer with C_1 symmetry has been observed with the ethyl group in perpendicular position to

the nominal phenyl plane [63]. Other studies on molecules related to 2EF where an ethyl group is attached to a double bond involving in a planar frame are those on propionaldehyde [31,32] and methyl propionate [64]. In propionaldehyde, the ethyl group also takes two possible positions, the in-plane *syn* [31] and the slightly higher in energy, out-of-plane *gauche* conformation where the tilt angle of the methyl group is 128.2° [32]. In methyl propionate, the strongest lines in the microwave spectrum belong to the most stable C_s conformer [64]. The *gauche* form has not been reported, but might also exist with less intensity in the spectrum [64].

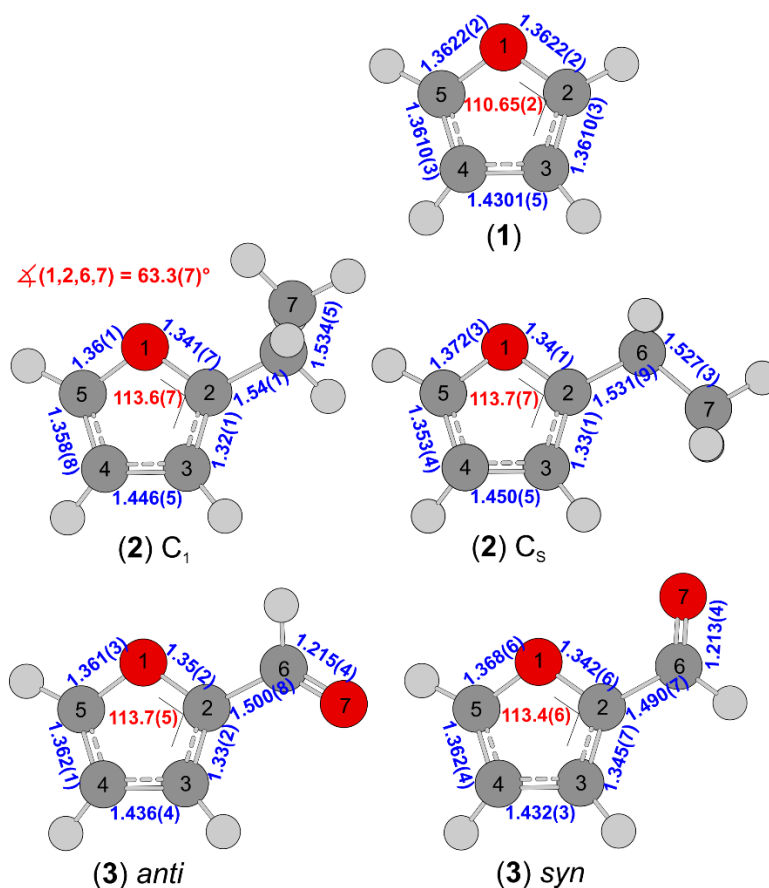


Figure 3. Comparison of some geometry parameters of (1) furan [8], (2) 2EF (this work), and (3) furfural [54]. The bond lengths given in blue are in Å; the bond angle $\angle(O1,C2,C3)$ given in red is in degree.

The potential energy curves calculated at the MP2/6-311++G(d,p) and MP2/6-31G(d,p) levels of theory presented in Figure 2 demonstrate that the C_1 conformer is lower in energy than the C_s conformer. However, the intensity observed in the microwave spectrum, as illustrated in

Figure 4, indicates that transitions of the C_s conformer are the more intense. Assuming that the dipole moment components are correctly calculated by *ab initio*, the similar values of μ_b predicted for the C_s and the C_1 conformer suggest lower intensity for transitions of the C_s conformer, which is about $2 \text{ kJ}\cdot\text{mol}^{-1}$ higher in energy than the C_1 conformer. Nevertheless, the experimental spectrum of the C_s conformer is clearly more intense than that of the C_1 conformer. In a study on methyl butyrate, Hernandez-Castillo et al. determined the rotational temperatures of two experimentally observed conformers with a Boltzmann plot by using the relationship between the integrated line intensities from the chirp-pulsed FTMW spectrum and the corresponding lower state energy [65]. The results showed slightly different rotational temperatures for the two conformers ($0.86 \pm 0.19 \text{ K}$ for the C_1 equivalent (g_{\pm},a) conformer vs. $0.35 \pm 0.08 \text{ K}$ for the C_s equivalent (a,a) conformer), indicating that the collisional cooling is conformer specific, with the C_s equivalent (a,a) conformer more efficiently cooled than the C_1 equivalent (g_{\pm},a) conformer [65]. If the same is true for 2EF, this might explain well the intensity behavior in contrast to the energy order of the C_s and the C_1 conformer. Quantitative statement on the conformational intensity and stability is not attempted due to the absence of dipole moment measurements and the lack of trust in intensity ratio of the current setup as well as in energy and dipole moment calculations.

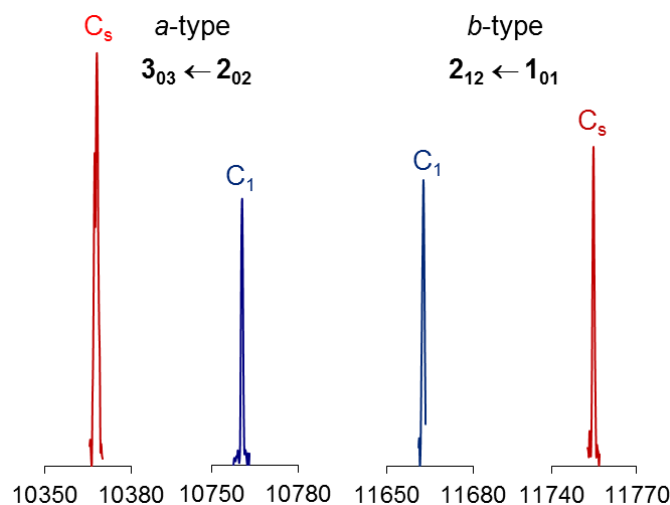


Figure 4. Some portions of the broadband scan of 2EF recorded by overlapping spectra with 50 co-added decays per each spectrum for comparing the intensity of the C_1 and the C_s conformer. The frequencies are in MHz. The intensities are given in arbitrary units and logarithm scale to visualize better the less intense lines of the C_1 conformer. The two left-hand side spectra correspond to the $3_{03} \leftarrow 2_{02}$ a -type transition of the two conformers, and the two right-hand side spectra to the $2_{12} \leftarrow 1_{01}$ b -type transition.

Conclusion

Using a combination of microwave spectroscopy and quantum chemical calculations, the jet-cooled spectra of two conformers (C_s and C_1) of 2EF and all their ^{13}C and ^{18}O -isotopologues were assigned and fitted to root-mean-square deviation close to experimental accuracy. The substitution r_s structure and semi-experimental equilibrium r_e^{SE} structures were determined using Kraitchman's equations, yielding accurate heavy atom coordinates, bond lengths, and bond angles. Comparing the bond lengths and the O1–C2–C3 bond angle of 2EF with those of furan and furfural indicates that the nature of the substituent is of minor importance for the structure of the furan ring, but the substitution increases the bond angle at the substituted position and consequently decreases the O1–C2 and C2–C3 bond lengths. For the C_1 conformer, the tilt angle of $63.3(7)^\circ$ of the methyl group out of the furan plane was compared with that of other molecules where an ethyl group is attached to a double bond involving in a planar frame. The intensity ratio observed in the microwave spectrum is the inverse of the energy order of the two conformers, suggesting that probably, the C_s conformer of 2EF is more efficiently cooled than the C_1 conformer.

Disclosure statement

No potential conflict of interest was reported by the authors.

Acknowledgments

The author thanks Prof. Dr. Wolfgang Stahl for providing the spectrometer for the measurements. This investigation on a semi-rigid rotor molecule is dedicated to Dr. Jon T. Hougen, and the author believes that he would enjoy reading this paper, the way he enjoyed seeing every equation coming out during the theory study of the author with him. This work was supported by the Agence Nationale de la Recherche ANR (project ID ANR-18-CE29-0011).

References

- [1] S. Yannai, (Ed.). (2003). Dictionary of Food Compounds with CD-ROM. New York: Chapman and Hall/CRC, <https://doi.org/10.1201/9781420068450>.
- [2] G. Mosciano, P&F 16 (1991) 49.
- [3] V. Van, C. Dindic, W. Stahl, H.V.L. Nguyen, ChemPhysChem 16 (2015) 291–294.
- [4] R. Hakiri, N. Derbel, H.V.L. Nguyen, H. Mouhib, Phys. Chem. Chem. Phys. 20 (2018) 25577–25582.

- [5] V. Van, W. Stahl, H.V.L. Nguyen, *ChemPhysChem* 17 (2016) 3223–3228.
- [6] T. Nguyen, C. Dindic, W. Stahl, H.V.L. Nguyen, I. Kleiner, *Mol. Phys.* (2019). DOI: 10.1080/00268976.2019.1668572.
- [7] V. Van, W. Stahl, M.T. Nguyen, H.V.L. Nguyen, *Can. J. Phys.* (2019). DOI: 10.1139/cjp-2019-0475
- [8] B. Bak, D. Christensen, W.B. Dixon, L. Hansen-Nygaard, J. Rastrup Andersen, M. Schottländer, *J. Mol. Spectrosc.* 9 (1962) 124–129.
- [9] V. Van, J. Bruckhuisen, W. Stahl, V. Ilyushin, H.V.L. Nguyen, *J. Mol. Spectrosc.* 343 (2018) 121–125.
- [10] I.A. Finneran, S.T. Shipman, S.L. Widicus Weaver, *J. Mol. Spectrosc.* 280 (2012), 27–33.
- [11] B. Bak, D. Christensen, J. Rastrup-Andersen, E. Tannenbaum, *J. Chem. Phys.* 25 (1956) 892.
- [12] V. Van, W. Stahl, H.V.L. Nguyen, *Phys. Chem. Chem. Phys.* 17 (2015) 32111–32114.
- [13] G.O. Braathen, K. Kveseth, C.J. Nielsen, K. Hagen, *J. Mol. Struct.* 145 (1986) 45–68.
- [14] B. Bak, D. Christensen, L. Hansen-Nygaard, J. Rastrup-Andersen, *J. Mol. Spectrosc.* 9 (1962) 222–224.
- [15] W. Jäger, H. Mäder, *Z. Naturforsch.* 42a (1987) 1405–1409.
- [16] W. Jäger, H. Mäder, *J. Mol. Struct.* 190 (1988) 295–305.
- [17] J.H. Griffiths, A. Wardley, V.E. Williams, N.L. Owen, J. Sheridan, *Nature* 216 (1967) 1301.
- [18] H.-W. Nicolaisen, J.-U. Grabow, N. Heineking, W. Stahl, *Z. Naturforsch.* 46a (1991) 635–638.
- [19] A. Kumar, J. Sheridan, O.L. Stiefvater, *Z. Naturforsch.* 33a (1978) 145–152.
- [20] H. Møllendal, A. Kononov, *J. Phys. Chem. A* 114 (2010) 2151–2156.
- [21] E. Fliege, H. Dreizler, M. Meyer, K. Iqbal, J. Sheridan, *Z. Naturforsch.* 41a (1986) 623–636.
- [22] O.L. Stiefvater, P. Nösberger, J. Sheridan, *Chem. Phys.* 9 (1975) 435–444.
- [23] E.R.L. Fliege, *Z. Naturforsch.* 45a (1990) 911–922.
- [24] E. Saegebarth, A.P. Cox, *J. Chem. Phys.* 43 (1965) 166.
- [25] L. Nygaard, R.L. Hansen, J.T. Nielsen, J. Rastrup-Andersen, G.O. Sørensen, P.A. Steiner, *J. Mol. Struct.* 12 (1972) 59–69.
- [26] J. Demaison, M.K. Jahn, E.J. Cocinero, A. Lesarri, J.-U. Grabow, J.-C. Guillemin, H.D. Rudolph, *J. Phys. Chem. A* 117 (2013) 2278–2284.
- [27] J. Makarewicz, S. Huber, B. Brupbacher-Gatehouse, A. Bauder, *J. Mol. Struct.* 612 (2002) 117.
- [28] K.-M. Marstokk, H. Møllendal, *J. Mol. Struct.* 23 (1974) 93–101.
- [29] D. Christen, J.H. Griffiths, J. Sheridan, *Z. Naturforsch.* 37a (1982) 1378–1385.
- [30] E. Gougoula, C. Medcraft, J. Heitkämper, N. R. Walker, *J. Chem. Phys.* 151 (2019) 144301.
- [31] S.S. Butcher, E.B. Wilson, Jr., *J. Chem. Phys.* 40 (1964) 1671.
- [32] J. Randell, J.A. Hardy, A.P. Cox, *J. Chem. Soc., Faraday Trans. 2*, 84 (1988) 1199–1212.
- [33] M. Hayashi, M. Adachi, J. Nakagawa, *J. Mol. Spectrosc.* 86 (1981) 129–135.
- [34] M. Adachi, J. Nakagawa, M. Hayashi, *J. Mol. Spectrosc.* 91 (1982) 381–388.
- [35] J.M. Riveros, E.B. Wilson, Jr., *J. Chem. Phys.* 46 (1967) 4605.
- [36] H. Mouhib, W. Stahl, *ChemPhysChem* 13 (2012) 1297–1301.

- [37] L. Ferres, W. Stahl, H.V.L. Nguyen, *Mol. Phys.* 114 (2016) 2788–2793.
- [38] L. Ferres, H. Mouhib, W. Stahl, H.V.L. Nguyen, *ChemPhysChem* 18 (2017) 1855–1859.
- [39] E.G. Schnitzler, N.A. Seifert, S. Ghosh, J. Thomas, Y. Xu, W. Jäger, *Phys. Chem. Chem. Phys.* 19 (2017) 4440–4446.
- [40] M.E. Sanz, S. Blanco, J.C. López, J.L. Alonso, *Angew. Chem.* 47 (2008) 6216–6220.
- [41] P. Ottaviani, B. Velino, W. Caminati, *Chem. Phys. Lett.* 428 (2006) 236–240.
- [42] J.-R. A. Moreno, D. Petitprez, T.R. Huet, *Chem. Phys. Lett.* 419 (2006) 411–416.
- [43] G.G. Brown, B.C. Dian, K.O. Douglass, S.M. Geyer, S.T. Shipman, B.H. Pate, *Rev. Sci. Instrum.* 79 (2008) 053103.
- [44] M.J. Frisch, G.W. Trucks, H.B. Schlegel, G.E. Scuseria, M.A. Robb, J.R. Cheeseman, G. Scalmani, V. Barone, G.A. Petersson, H. Nakatsuji, X. Li, M. Caricato, A.V. Marenich, J. Bloino, B. G. Janesko, R. Gomperts, B. Mennucci, H.P. Hratchian, J.V. Ortiz, A.F. Izmaylov, J.L. Sonnenberg, D. Williams-Young, F. Ding, F. Lipparini, F. Egidi, J. Goings, B. Peng, A. Petrone, T. Henderson, D. Ranasinghe, V.G. Zakrzewski, J. Gao, N. Rega, G. Zheng, W. Liang, M. Hada, M. Ehara, K. Toyota, R. Fukuda, J. Hasegawa, M. Ishida, T. Nakajima, Y. Honda, O. Kitao, H. Nakai, T. Vreven, K. Throssell, J.A. Montgomery, Jr., J. E. Peralta, F. Ogliaro, M.J. Bearpark, J.J. Heyd, E.N. Brothers, K.N. Kudin, V.N. Staroverov, T.A. Keith, R. Kobayashi, J. Normand, K. Raghavachari, A.P. Rendell, J.C. Burant, S.S. Iyengar, J. Tomasi, M. Cossi, J.M. Millam, M. Klene, C. Adamo, R. Cammi, J.W. Ochterski, R.L. Martin, K. Morokuma, O. Farkas, J.B. Foresman, D.J. Fox, *Gaussian 16*, Revision B.01, Inc., Wallingford CT, 2016.
- [45] J.-U. Grabow, W. Stahl, H. Dreizler, *Rev. Sci. Instrum.* 67 (1996) 4072–4084.
- [46] J.-U. Grabow, W. Stahl, *Z. Naturforsch.* 45a (1990) 1043–1044.
- [47] V. Van, W. Stahl, H.V.L. Nguyen, *J. Mol. Struct.* 1123 (2016) 24–29.
- [48] R. Hakiri, N. Derbel, W.C. Bailey, H.V.L. Nguyen, H. Mouhib, *Mol. Phys.* (2020). DOI: 10.1080/00268976.2020.1728406.
- [49] J. Kraitchman, *Am. J. Phys.* 21 (1953) 17–24.
- [50] Z. Kisiel, PROSPE-Programs for ROTational SPEctroscopy, available at <http://info.ifpan.edu.pl/~kisiel/prospe.htm>.
- [51] C.C. Costain, *Trans. Am. Crystallogr. Assoc.* 2 (1966) 157–164.
- [52] J. Demaison, A. G. Császár, L.D. Margulès, H.D. Rudolph, *J. Phys. Chem. A* 115 (2011) 14078.
- [53] B.J. Esselman, B.K. Amberger, J.D. Shutter, M.A. Daane, J.F. Stanton, R.C. Woods, R.J. McMahon, *J. Chem. Phys.* 139 (2013) 224304.
- [54] S. Herbers, P. Kraus, J.-U. Grabow, *J. Chem. Phys.* 150 (2019) 144308.
- [55] Z. Kisiel, *J. Mol. Spectrosc.* 218 (2003) 58–67.
- [56] R.A. Motiyenko, E.A. Alekseev, S.F. Dyubko, F.J. Lovas, *J. Mol. Spectrosc.* 240 (2006) 93–101.
- [57] K.-M. Marstokk, H. Møllendal, *Acta Chem. Scand.* 46 (1992) 923–927.
- [58] K. Toshio, O. Teruhiko, M. Shiro, *Chem. Lett.* 5 (1976) 607–610.

- [59] K.-M. Marstokk, H. Møllendal, *Acta Chem. Scand.* 48 (1994) 25–31.
- [60] K.-M. Marstokk, H. Møllendal, *Acta Chem. Scand.* 48 (1994) 298–305.
- [61] R.G. Latypova, L.Y. Gubaidullin, U.M. Dzhemilev, N.M. Pozdeev, *Zh. Strukt. Khim.* 21 (1980) 197.
- [62] I. Hedgecock, N.W. Larsen, L. Nygaard, T. Pedersen, G.O. Sørensen, *J. Mol. Struct.* 223 (1990) 33–44.
- [63] W. Caminati, D. Damiani, G. Corbelli, B. Velino, C.W. Bock, *Mol. Phys.* 74 (1991) 885–895.
- [64] H.V.L. Nguyen, W. Stahl, I. Kleiner, *Mol. Phys.* 110 (2012) 2035–2042.
- [65] A.O. Hernandez-Castillo, C. Abeysekera, B.M. Hays, I. Kleiner, H.V.L. Nguyen, T.S. Zwier, *J. Mol. Spectrosc.* 337 (2017) 51–58.